EasyChair Preprint

№ 15181

DEM-Based Analysis and Optimization of an Excavation Bucket Drum for In-Situ Resource Utilization

Tomoyasu Nakano, Takuya Omura and Genya Ishigami

September 30, 2024

4213 | DEM-Based Analysis and Optimization of an Excavation Bucket Drum for In-Situ Resource Utilization

Tomoyasu Nakano [a,*], Takuya Omura [a], Genya Ishigami [a]

[a] *Department of Mechanical Engineering, Keio University, Japan*

** Corresponding author: nakano.tomoyasu@keio.jp*

A B S T R A C T

Lunar infrastructure construction involves leveling of the lunar surface and collecting lunar regolith as a building material. RASSOR 2.0 developed by NASA is one of the typical robotic vehicles as a lunar excavator. It features cylindrical rotating bucket drums for collecting regolith, positioning it as a pivotal tool for future lunar in-situ resource utilization and infrastructure development. However, the optimization of the bucket drum's shape and its motion remain as open issue. Therefore, this study aims to find an optimal design of the bucket drum through numerical simulation using the discrete element method (DEM). We introduce five key design parameters of the bucket drum: two of them are related to the bucket shape (scoop throat length, scoop inlet number) and the rest of them are to motion (bucket vertical force, horizontal velocity, and angular velocity). These five parameters were examined in accordance with two performance indices: the sand fill ratio in the drum and the power consumption of the excavation. Solving the multi-objective problem of increasing the fill ratio and reducing power consumption, we found an optimal bucket drum shape and motion. Subsequently, a bucket drum reflecting the optimal shape was fabricated, and the optimal motion was tested. The test results qualitatively matched with the results derived from the DEM analysis. This outcome highlights the validity of the relationship between the design parameters and two performance indices.

Keywords
In-situ Resource Utilization
Bucket Drum
DEM Simulation
Excavation Efficiency

1. Introduction

The necessity of lunar infrastructure development is expected to be a critical focus in the coming years. The lunar surface, characterized by its uneven terrain due to frequent meteor impacts, poses significant challenges for base construction at proposed sites. Jehn et al. (2023) lists three primary stages: clearing, grading, and compaction for effective construction site preparation. Clearing involves the removal of rocks and obstacles, grading adjusts the terrain to flatten the site, and compaction increases the soil density to provide a stable foundation for further construction. Especially, the processes of clearing and grading are crucial for removing the irregularities caused by craters, emphasizing the essential role of lunar excavators in these tasks.

To establish a sustainable human activity on the moon in the future, in-situ resource utilization (ISRU) is paramount. ISRU practices involve the direct utilization of local resources, such as extracting essential elements like oxygen, hydrogen, titanium, aluminum, and iron from lunar soil, also known as regolith (Grant et al., 1991). These resources are for various applications including rocket fuel, life support systems, and residential modules. (Mueller, 2023). Crucially, the collection of regolith is a fundamental step towards enabling sustained lunar activities, thereby making lunar excavators indispensable.

Responding to this need, a significant advancement has been made with NASA's Regolith Advanced Surface Systems Operations Robot (RASSOR 2.0), designed specifically for the low-gravity conditions of lunar environments (Mueller et al., 2016). As shown in Fig. 1, this robot incorporates rotating bucket drums equipped with digging scoops, which trap regolith inside the drum. Bucket drums offer a superior balance of efficiency, simplicity, and adaptability compared to traditional excavation methods, making them particularly well-suited to the unique challenges posed by lunar regolith and low-gravity environments. The design engages only 1-2 scoops at a time, minimizing resistive forces and reducing energy consumption (Clark, 2009). In contrast, traditional methods such as shovels and bulldozers, which rely heavily on gravity and pulling forces, face significant challenges in low-gravity conditions, including the risk of equipment overturning due to high reactive forces. Bucket drums circumvent these issues by employing lower excavation forces and maintaining minimal contact with the regolith. Thus, the RASSOR 2.0's capability to excavate and transport regolith is vital for ISRU processes, highlighting its role in infrastructure development and lunar resource extraction strategies. However, the optimization study of the shape and motion of the bucket drums has yet to be accomplished.

Fig. 1. RASSOR 2.0 by NASA

https://doi.org/10.56884/ABCD1234 *(ed. note: ISTVS will update your paper's DOI)*
ISBN 978-1-942112-57-0

In this research, we exploit the discrete element method (DEM) to analyze the behavior of sand particles and optimize the shape and motion. Our study introduces five key design parameters: scoop throat length, scoop inlet number, bucket vertical force, horizontal velocity, and angular velocity. These parameters were evaluated based on two performance indices: the sand fill ratio in the drum and the power consumption of the excavation. By addressing this multi-objective problem, we identified an optimal bucket drum configuration that achieves a favorable balance between the fill ratio and power consumption compared to other configurations. Subsequently, experimental testing was conducted to evaluate the DEM results against the measured fill ratio and energy consumption results.

2. Selection of shape and motion parameters

2.1. Optimization function for bucket drums

To achieve the efficient excavation of lunar regolith, two primary optimization criteria were established: fill ratio, R and energy consumption, E. These criteria are essential for maximizing the amount of sand collected per excavation cycle while minimizing the energy required, thus ensuring the efficiency and sustainability of lunar operations.

The fill ratio is defined as the volume of sand collected inside the bucket drum divided by the total volume of the drum. Maximizing fill ratio is crucial for improving the efficiency of each excavation cycle. The fill ratio R is given as:

$$R = V_{\text{sand}}/V_{\text{drum}} \tag{1}$$

where V_{sand} is the volume of sand collected and V_{drum} is the total volume of the bucket drum.

Energy consumption during excavation is a critical factor due to the limited power supply available for lunar missions. In this study, energy consumption is calculated based on the energy required for three main actions: rotating the bucket drum, pushing it vertically into the sand, and advancing it horizontally. Vertical pushing energy involves the energy required to press the bucket drum into the sand. Rotational energy pertains to the energy needed to turn the bucket drum to scoop the sand. Horizontal advancement energy accounts for the energy consumed as the bucket drum moves forward through the sand.

2.2. Selection of key parameters

The shape and motion parameters of the bucket drum are critical to its performance. Five key parameters are selected for optimization: two shape parameters (scoop throat length, N_r and scoop inlet number, N_θ) and three motion parameters (vertical force, F, horizontal velocity, v, and angular velocity, ω), as listed in Table 1.

The scoop throat length, N_r, which determines the amount of sand captured in each scoop, is defined as:

$$N_r = r_{\text{in}}/r \tag{2}$$

where r_{in} is the scoop height and r is the radius of the bucket drum, as shown in Fig. 2(a).

The scoop inlet number, N_θ, which impacts the frequency of sand scooping, is given as:

$$N_\theta = 2\pi/\theta \tag{3}$$

Table 1
Five key parameters for drum design and motion

Type	Parameter	Symbol	Unit
Shape	Scoop throat length	N_r	[−]
	Scoop inlet number	N_θ	[−]
Motion	Vertical force	F	[N]
	Horizontal velocity	v	[m/s]
	Angular velocity	ω	[rad/s]

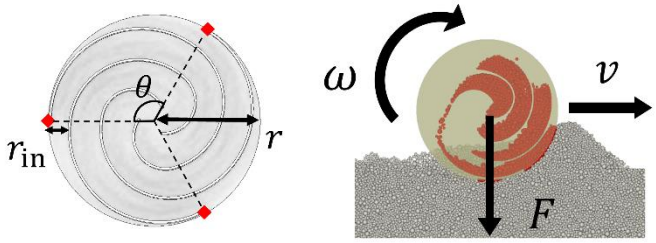

(a) Two design parameters *(b) Three motion parameters*
Fig. 2. Side view of bucket drum with five key parameters

Table 2
Discrete element method parameters for Toyoura sand

Density [g/cm^3]	2.663	
Diameter [μm]	215, 260, 311, 395, 470	
Mass ratio [%]	18.6, 32.5, 23.7, 15.8, 9.3	
Young's modulus [MPa]	20	
Poisson's ratio [−]	0.3	
Rolling resistance [−]	0.3	
	Particle-particle	Particle-bucket drum
Static friction coefficient [−]	0.5	0.3
Dynamic friction coefficient [−]	0.5	0.3
Restitution coefficient [−]	0.5	0.3

where θ is the angle between adjacent scoops. Increasing the number of scoops can enhance the fill ratio but may also increase the energy consumption.

The three motion parameters shown in Fig. 2(b) are essential for the drum's excavation function. The vertical force, F ensures that the drum maintains contact with the sand. The horizontal velocity, v corresponds to the forward movement of the excavator. The angular velocity of the drum, ω is correlated with the horizontal velocity. Optimizing these motion parameters ensures that the bucket drum operates efficiently and effectively under lunar conditions, maintaining a high fill ratio while minimizing energy consumption.

3. DEM simulations for optimization

This section focuses on optimizing the bucket drum's design and motion parameters using the DEM to maximize the fill ratio and minimize energy consumption. The optimization process involves varying two key shape parameters and three key motion parameters of the bucket drum. Initially, we optimized the two shape parameters (N_r and N_θ), followed by the optimization of the three motion parameters (F, v, and ω).

3.1. DEM excavation model setup

Commercial software Ansys Rocky DEM (Ansys Inc., 2023) was used for the analysis. In the DEM simulations, it is crucial to set the parameters for particles accurately. This study utilized the

parameters for Toyoura sand provided by S. Ozaki et al. (2023), listed in Table 2. Toyoura sand is frequently employed to simulate and analyze soil behavior in the field of Terramechanics. To reproduce the particle size distribution similar to actual Toyoura sand within DEM, five representative diameters and their corresponding mass ratios were selected based on the particle size selection method by Omura et al. (2023). Details of the selection process are provided in Appendix A. Note that the particle size was scaled up by a factor of 10 in the DEM simulations to reduce computational cost. To facilitate comparison with Earth-based testing, gravity was set to 9.81 m/s^2. The bucket drum had a radius of 100 mm, a width of 50 mm, and a scoop thickness of 2 mm. The drum's mass was calculated using a density of 2000 kg/m^3, based on the carbon fiber material used in the RASSOR 2.0.

In addition to setting particle parameters, selecting suitable contact models is essential for DEM simulations. The contact forces in DEM consist of two main components: forces normal to the contact plane and forces tangential to the contact plane. This study employs the Hertzian spring-dashpot model for the normal forces and the Mindlin-Deresiewicz model for the tangential forces. These models represent the interactions between particles, as well as between particles and equipment, contributing to the simulation results.

3.2. Shape optimization via DEM

During the DEM simulation, the bucket drum undergoes three rotations to fully evaluate the relationship between the fill ratio and energy consumption. Combinations of the scoop throat length, N_r and the scoop inlet number, N_θ that satisfy the six constraints are listed in Table 3.

To ensure fair optimization conditions, constraints were imposed on the spiral shape inside the bucket drum while varying the scoop throat length, N_r and the number of scoops, N_θ. Six constraints were established:

1. The spiral structure must complete one full 360° turn around the axis of the bucket drum.
2. The distance from the inner end of the scoop to the center of the drum, r_{ctr} must be 0.2 times the radius, r.
3. The radius of curvature, r_{cvt} from the scoop tip to the adjacent scoop must be formulated with respect to the scoop throat length, N_r as:

$$r_{\mathrm{cvt}} = r - \frac{r_{\mathrm{in}} + h}{2} = r - \frac{rN_r + h}{2} \tag{4}$$

   where h denotes the thickness of the scoop.
4. The spiral structure must pass through points that divide the line connecting the scoop tip and the center of the drum into $N_\theta - 1$ equal segments, ensuring consistent spacing and alignment of the scoops.
5. A tangential constraint must be used to maintain a point of tangency when connecting two curves that form the spiral structure, ensuring that the transition between curves is smooth.
6. The minimum spacing, l between the scoops must satisfy $l/r \geq 0.1$, preventing clogging and maintaining smooth operation.

Initially, nine combinations of N_r $(= 0.1, 0.2, 0.3)$ and N_θ $(= 2, 3, 4)$ were analyzed to gain insights into the relationship between the fill ratio and energy consumption. Figure 3 shows the relationship between energy consumption, E and fill ratio, R for these combinations. It was confirmed that larger values of N_r and N_θ result in lower energy consumption and higher fill ratio, with the influence of the scoop throat length being more pronounced.

Table 3
Constraint-satisfying design parameters

	$N_\theta = 2$	$N_\theta = 3$	$N_\theta = 4$	$N_\theta = 5$
$N_r = 0.1$	✓	✓	✓	✓
$N_r = 0.2$	✓	✓	✓	✓
$N_r = 0.3$	✓	✓	✓	N/A
$N_r = 0.4$	✓	✓	N/A	N/A
$N_r = 0.5$	✓	N/A	N/A	N/A
$N_r = 0.6$	✓	N/A	N/A	N/A

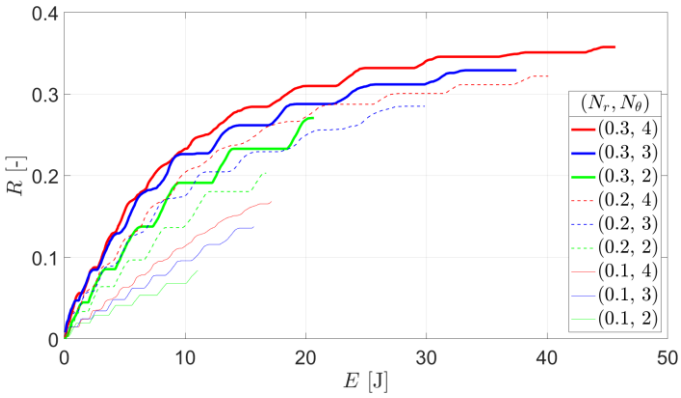

Fig. 3. Energy vs. fill ratio under different drum shapes (9 types)

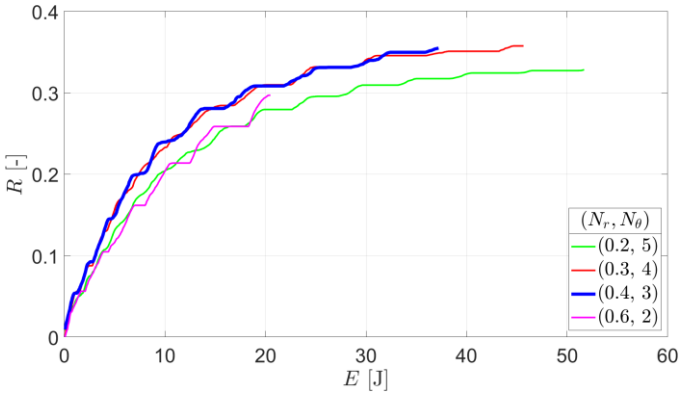

Fig. 4. Energy vs. fill ratio under different drum shapes (4 types)

Based on these results, the shape optimization of the bucket drum was conducted for combinations with the maximum N_r values that satisfy the constraints for each N_θ $(= 2, 3, 4, 5)$. Figure 4 illustrates the corresponding energy consumption and fill ratio. The optimal design was determined to be $(N_r, N_\theta) = (0.4, 3)$ due to its favorable balance of a high fill ratio and low energy consumption, as indicated by the blue line in Fig. 4. The combination $(N_r, N_\theta) = (0.3, 4)$, shown with the red line, has a similar result but was found less optimal due to manufacturing difficulties, higher risk of sand clogging, and increased production costs associated with more blades. Consequently, $(N_r, N_\theta) = (0.4, 3)$ was selected as the optimal set of shape parameters.

3.3. Experimental design for motion parameters

The experimental design method efficiently extracts accurate information from a limited number of experiments. This method was applied to the three motion parameters: vertical force, F, horizontal velocity, v, and angular velocity, ω. The Box-Behnken

Design (BBD) was selected to determine the optimal combination of motion parameters to minimize energy consumption and maximize fill ratio.

BBD, a statistical method introduced by Box and Behnken (1960), used for the optimization of multiple variables with minimal experimentation. This design is particularly advantageous as it requires fewer experimental runs compared to other methods, while still providing comprehensive insights into the interactions between variables (Yıldız, 2022). BBD effectively fits a second-order polynomial model to the data, allowing for accurate predictions and optimizations. Each factor is set to three levels: low (-1), medium (0), and high $(+1)$. The number of experiments, N is given by: $N = 2k(k-1) + c_p$ where k is the number of factors and c_p is the number of center points. Table 4 lists the three levels for each of the three factors. For this study, with four center points, the total number of experiments was set to 16.

3.4. Motion optimization via DEM

To analyze the impact of the motion parameters on the bucket drum's performance, specifically fill ratio and energy consumption, regression analysis was performed using MATLAB's 'fitlm' function, including second-order terms for the three motion parameters. This model accounts for the squared terms of each parameter as well as the interaction terms between parameters. This approach enables the identification of complex interactions and nonlinear effects among the parameters, providing deeper insights into their interdependencies.

Data on the fill ratio and energy consumption were collected at the 16 experimental points to construct each regression model. The regression model for the maximum fill ratio, $R_{\max}$ is given by:

$$\begin{aligned} R_{\max} = {} & 0.10 + 0.031F + 5.9v - 0.10\omega - 0.20Fv \\ & -0.0011F\omega - 2.9v\omega + 0.0013F^2 - 170v^2 \\ & -0.045\omega^2 \end{aligned} \tag{5}$$

As observed from Figs. 3 and 4, the energy consumption, E, versus the fill ratio, R, curve can be approximated by a first-order system response. The approximation equation is defined as follows:

$$R = R_{\max}\left(1 - \exp(-E/\tau)\right) \tag{6}$$

In this context, the coefficient τ is defined as the value of energy consumption at which the fill ratio reaches 63.2 % of its maximum value, $R_{\max}$. Therefore, τ evaluates the change rate of energy consumption until the fill ratio stabilizes. Thus, we conducted an optimization of the three motion parameters aimed at minimizing the time constant while simultaneously maximizing the maximum fill ratio. The regression model for the time constant, τ is given by:

$$\begin{aligned} \tau = {} & 2.7 + 1.0F + 65v - 1.2\omega + 18Fv + 0.76F\omega \\ & -69v\omega + 0.018F^2 - 363v^2 + 0.93\omega^2 \end{aligned} \tag{7}$$

Table 4
Box-Behnken design factor levels for motion parameters

Coding	Factors		
	F [N]	v [m/s]	ω [rad/s]
+1	10	0.04	−0.6
0	5	0.02	−1.2
−1	0	0	−1.4

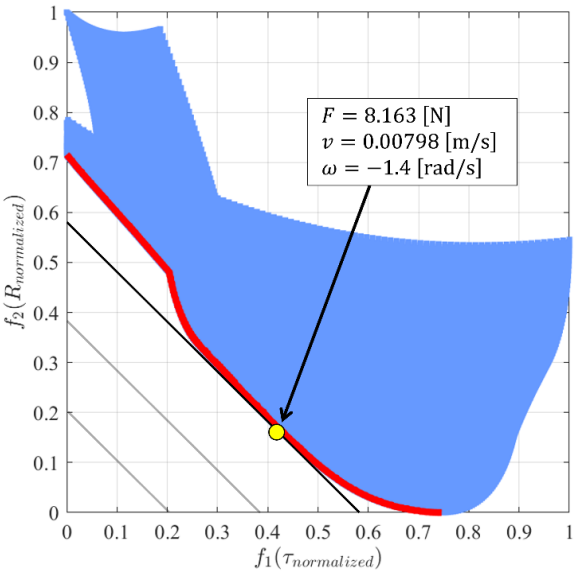

Fig. 5. Feasible region and pareto frontier with optimal solution when $w_1 = w_2 = 0.5$

To minimize the value of τ and maximize the maximum fill ratio, a multi-objective optimization was performed to find the optimal combination of vertical force, F, horizontal velocity, v, and angular velocity, ω. The motion parameters were explored within the range of upper and lower limits set in Table 4. Equation 5 was substituted into Eq. 9 as f_2 and Eq. 7 into Eq. 10 as f_1 to normalize the time constant and maximum fill ratio as follows:

$$\text{minimize} \quad w_1 f_1 + w_2 f_2 \tag{8}$$

$$\text{s.t.} \quad f_1 = \frac{\tau - \tau_{\min}}{\tau_{\max} - \tau_{\min}} \tag{9}$$

$$f_2 = 1 - \frac{R_{\max} - (R_{\max})_{\min}}{(R_{\max})_{\max} - (R_{\max})_{\min}} \tag{10}$$

Figure 5 shows the plot of the normalized time constant, f_1 versus the normalized fill ratio, f_2 as the three motion parameters are varied within the specified range. The blue region represents the set of feasible solutions, while the red curve represents the Pareto frontier. Each point on the Pareto frontier is a Pareto optimal solution (solution to the multi-objective optimization problem), having a trade-off with each other. Using the weighted sum method, the optimal solution is uniquely determined *by minimizing* the weighted sum in Eq. 8, where the weights w_1 and w_2 sum to 1. In this study, the weights for the fill ratio and energy consumption were set equally, with $w_1 = w_2 = 0.5$.

Figure 5 highlights the point on the Pareto frontier with yellow that corresponds to the minimum value that satisfies Eq. 8 under the given weights. The motion parameters at this point are $F = 8.163$ N, $v = 0.00798$ m/s, and $\omega = -1.4$ rad/s, representing the optimal solution of this study.

4. Experimental verification

This section focuses on the experimental verification of the optimal shape and motion parameters of the bucket drum determined through DEM simulations. The goal is to integrate insights obtained from excavation experiments to validate the

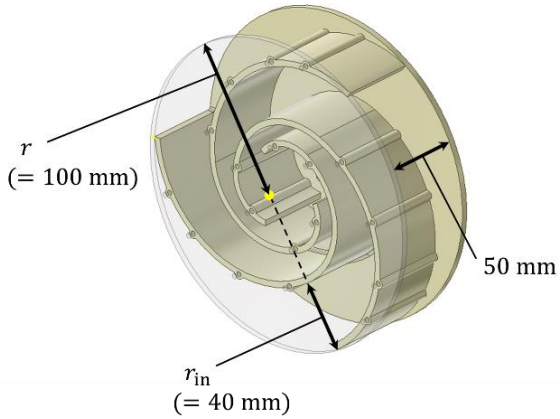

Fig. 6. CAD model with the scoop throat length and width of bucket drum for 3D printing

DEM simulation results. This section outlines the experimental setup and analysis methods used to achieve this goal.

4.1. Excavation experiment setup

Based on the optimal shape parameters, scoop throat length, $N_r = 0.4$, and number of scoops, N_θ=3, identified in Section 3, the CAD model of the bucket drum was created for 3D printing. Using the CAD model shown in Fig. 6, the bucket drum was 3D-printed with ABS-like resin due to its high bending strength, durability, and smooth surface, which reduces friction with the sand. One side of the drum was fabricated using a laser-cut acrylic plate. The transparent acrylic allowed for the observation of the behavior of the sand being trapped inside.

The experiments were conducted using an excavation test apparatus available in our laboratory. Figure 7 shows the apparatus, featuring a storage bin with dimensions of 3 m in length, 0.96 m in width, and 0.4 m in height filled uniformly with Silica sand No. 5. A camera was installed to capture the bucket drum's side view, allowing continuous monitoring of the sand fill status inside the drum during the experiment.

The optimal motion parameters obtained from DEM analysis were used for the experiments: a vertical force $F = 8.163$ N, a horizontal velocity $v = 0.00798$ m/s, and an angular velocity $\omega = -1.4$ rad/s. The bucket drum was rotated three times, and the relationship between the fill ratio and energy consumption was measured.

4.2. Analysis method

To quantify the amount of sand excavated inside the bucket drum during its rotation, a series of image processing techniques were employed. The procedure began with extracting the saturation component from the color images to remove dullness and disturbances. Next, the "imfindcircles" function in MATLAB was used to detect the bucket drum's position in the images. Following this, the detected bucket drum images were converted to grayscale and binarized using the Sobel operator to highlight edges. Subsequently, dilation processing and noise removal were applied using a median filter to enhance sand recognition. Finally, the volume of sand was estimated by counting the number of white pixels in the binarized images. Figure 8 illustrates the result of the image analysis, showing the detected area of sand inside the bucket drum.

The actuator (HEBI Robotics, X5-9) installed for the drum rotation provided the time-series data on current and voltage,

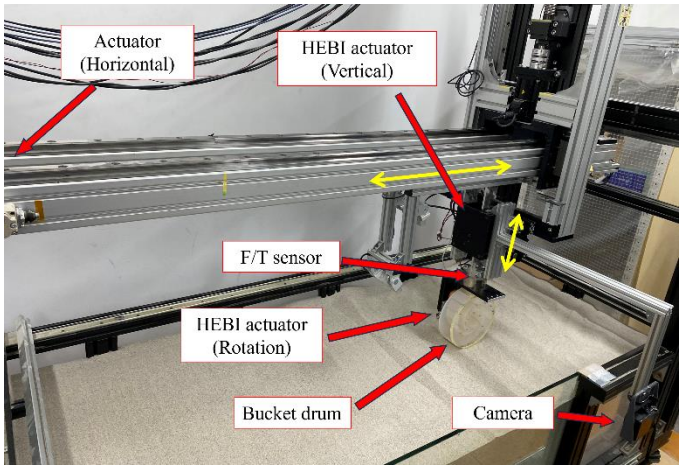

Fig. 7. Test apparatus for evaluating bucket drum excavation performance

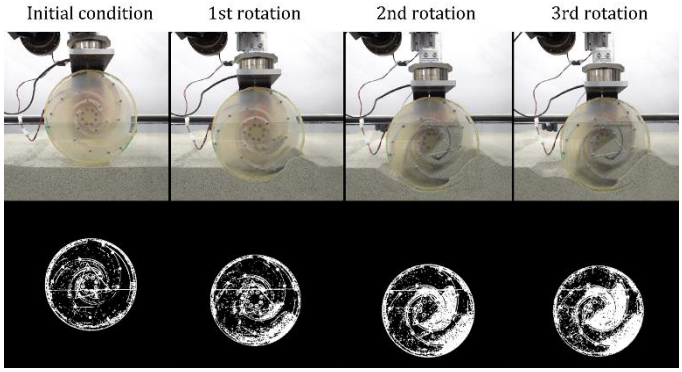

Fig. 8. Sequential visualization of the rotating bucket drum: real-time operation (top row), image processing analysis (bottom row)

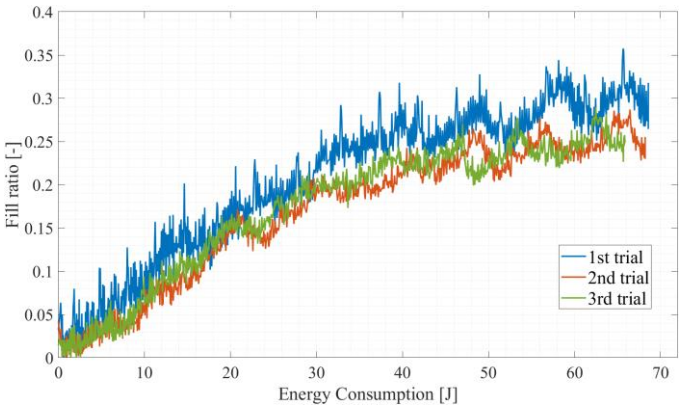

Fig. 9. Relationships between energy consumption and fill ratio in three excavation trials

which were used to calculate the energy consumption. The energy consumption was obtained by integrating the power, the product of current and voltage, over time.

4.3. Results and discussion

Figure 9 shows the relationship between energy consumption and fill ratio from the experiments three times, exhibiting a first-order system response, consistent with the DEM simulation results. This confirms a qualitative correlation between the experimental and DEM simulation results. However, the fill ratio measured from the experiments was slightly lower than that

obtained from the DEM simulations. This quantitative difference could be due to several reasons. First, the image processing techniques used may not capture all the sand particles accurately, leading to an underestimation of the fill ratio. Additionally, the experiments used Silica sand No. 5, while the DEM simulations used Toyoura sand. The larger particle size of Silica sand No. 5 compared to Toyoura sand could affect the fill ratio. Overall, experimental results highlight the effectiveness of using DEM for initial design optimization. By leveraging DEM simulations, a balance between fill ratio and energy consumption can be achieved, reducing the need for extensive physical prototyping. This approach not only saves time and cost but also provides a reliable method for evaluating new design concepts and motion parameters before actual implementation.

5. Conclusions and future work

This study investigated the optimization of the excavation bucket drum's shape and motion parameters using DEM simulations, supported by experimental verification. The parameters were evaluated based on two key performance indices: the sand fill ratio in the drum and the power consumption during excavation. Handling a multitude of parameters with varying potential values poses significant challenges, particularly when striving to balance these two indices. This study found that, in simulations, the relationship between energy consumption and fill ratio follows a first-order system response, a result that was also confirmed experimentally.

Our multi-objective optimization approach, which integrated DEM simulations with statistical methods like the Box-Behnken Design, proved essential in navigating these complexities. This approach facilitated a comprehensive exploration of design possibilities, ensuring that the optimal configuration was identified without extensive physical prototyping, thereby saving both time and resources. Leveraging DEM allows researchers to explore and refine various design options before committing to physical prototypes, leading to significant time and cost savings.

Future work will involve the integration of the optimized bucket drum with a lunar rover system, assessing its performance in a fully operational scenario. Additionally, enhancements to the DEM simulation environment, such as simulating excavation of the bucket drum in lunar conditions, will be undertaken. This will provide a more comprehensive understanding of the bucket drum's performance in realistic lunar scenarios.

6. Declaration of competing interest

The authors declare that they have no known competing financial interests or personal relationships that could have appeared to influence the work reported in this paper.

7. References

ANSYS, Inc., 2023. Rocky Technical Manual, Release 2023 R2. ANSYS, Inc., Southpointe, Canonsburg, PA.

Box, G.E.P., Behnken, D.W., 1960. Some new three level designs for the study of quantitative variables. Technometrics 2(4), 455–475.

Clark, D.L., Patterson, R.R., Wurts, D.W., 2009. A novel approach to planetary regolith collection: the bucket drum soil excavator. In: AIAA Space 2009 Conference & Exposition, pp. 6430.

Grant, H.D., Vaniman, D.T., French, B.M. (Eds.), 1991. Lunar sourcebook: A user's guide to the Moon. No. 1259. Cup Archive.

Jehn, I., Dreyer, C.B., van Susante, P.J., Primeau, J., 2023. Lunar site preparation requirements for construction of infrastructure elements. ASCEND 2023.

Mueller, R.P., 2023. A review of extra-terrestrial regolith excavation concepts and prototypes. Earth and Space 2022.

Mueller, R.P., Smith, J.D., Schuler, J.M., Nick, A.J., Gelino, N.J., Leucht, K.W., Dokos, A.G., 2016. Design of an excavation robot: regolith advanced surface systems operations robot (RASSOR) 2.0. In: 15th Biennial ASCE Conference on Engineering, Science, Construction, and Operations in Challenging Environments, Reston, VA, pp. 163-174. American Society of Civil Engineers.

NASA, 2020. NASA regolith Advanced Surface Systems Operations Robot (RASSOR) bucket drum design challenge. NASA. https://www.nasa.gov/general/nasa-regolith-advanced-surface-systems-operations-robot-rassor-bucket-drum-design-challenge/ (accessed on 2024-05-16).

Omura, T., Hamasaki, R., Ishigami, G., 2023. Gravitational dependency analysis on adhesive force of granular material using a discrete element method. In: Proceedings of the Japan Society of Microgravity Application.

Ozaki, S., Ishigami, G., Otsuki, M., Miyamoto, H., Wada, K., Watanabe, Y., Kobayashi, T., 2023. Granular flow experiment using artificial gravity generator at International Space Station. npj Microgravity 9(1), 61.

Yıldız, A., Uğur, L., Parlak, İ.E., 2022. Optimization of the cutting parameters affecting the turning of AISI 52100 bearing steel using the Box-Behnken experimental design method. Appl. Sci. 13(1), 3.

Appendix A

The selection of five representative particle diameters and their corresponding mass ratios for the DEM simulations was guided by a Gaussian mixture model, as described by Omura et al. (2023). This method ensures that the simulated distribution closely aligns with the observed characteristics of Toyoura sand.

The Gaussian mixture model employed two components to capture the distinct peaks in the particle size distribution observed by Ozaki et al. (2023). The five representative diameters were derived using the mean μ_i and standard deviation σ_i of these Gaussian components:

$$\begin{aligned} d_1 &= \mu_1 - \sigma_1 \\ d_2 &= \mu_1 \\ d_3 &= \pi_1(\mu_1 + \sigma_1) + \pi_2(\mu_2 - \sigma_2) \\ d_4 &= \mu_2 \\ d_5 &= \mu_2 + \sigma_2 \end{aligned} \tag{A.1}$$

where π_1 and π_2 represent the mixture ratios of the two Gaussian components. The third representative diameter d_3 was determined by weighting the difference $\mu_1 + \sigma_1$ and the sum $\mu_2 - \sigma_2$ using the mixture ratios. This calculation was crucial for balancing the overlapping regions of the two components, thereby preventing an overemphasis on any particular range within the distribution. Figure A.1 illustrates the five representative diameters and mass ratios, as determined by this selection method. This approach reduces the number of diameters, thereby lowering computational costs while maintaining the complexity of particle interactions in the simulations.

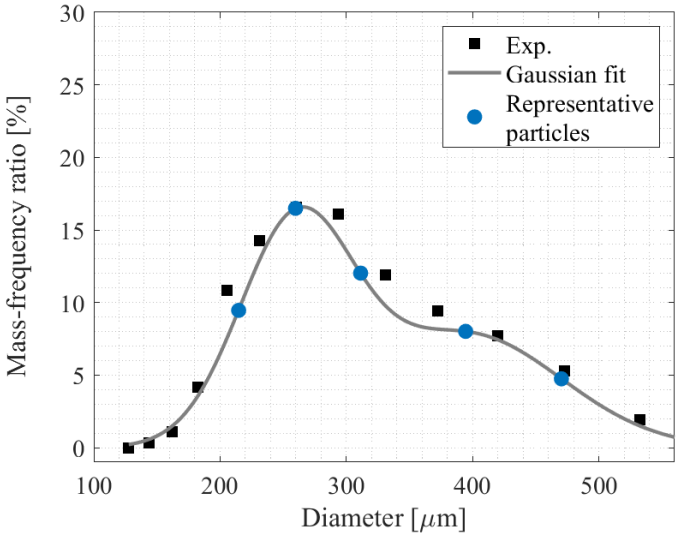

Fig. A.1. Fitting by Gaussian mixture model